

**VERIFICATION OF RESPONSE SPECTRAL SHAPES  
AND ANCHOR POINTS FOR DIFFERENT SITE CATEGORIES  
FOR BUILDING DESIGN CODES**

Walt Silva<sup>1</sup> and Gabriel Toro<sup>2</sup>  
Pacific Engineering and Analysis, El Cerrito, California<sup>1</sup>  
Risk Engineering Inc., Boulder, Colorado<sup>2</sup>

**ABSTRACT**

The dramatic increase in strong ground motion recordings over the last several years has provided both the impetus and opportunity to empirically examine the seismic design criteria in both the UBC and NEHRP code provisions. In this project both spectral design shapes and the usefulness of two spectral anchors are investigated using a comprehensive strong motion database and updated empirical attenuation relations. For the shapes, the results suggest that both the UBC and NEHRP design spectra provide enveloping criteria (except for site D at short periods) including cases for sites within 10 km of the fault rupture surface. For the NEHRP design spectra, comparison of the  $F_a$  and  $F_v$  factors to those implied by a recently developed empirical attenuation relation suggest that the NEHRP  $F_a$  factors may reflect too little nonlinearity while the  $F_v$  factors may show too much nonlinearity. Comparisons of the code shapes to the results from probabilistic seismic hazard analyses indicate that the fixed UBC shape has a moderate tendency to under-predict amplitudes for  $T > 1$  sec in places like San Francisco and Sacramento where large ( $M > 7$ ) earthquakes dominate the hazard at these periods. The more flexible NEHRP shape avoids this problem, but requires the specification of two anchoring points.

**INTRODUCTION**

Local geologic conditions have long been recognized to have a large effect upon strong ground motions. Del Barrio, in the 1855 Proceedings of the University of Chile states<sup>1</sup> "...a movement... must be modified while passing through media of different constitutions. Therefore, the earthquake effects will arrive to the surface with higher or lesser violence according to the state of aggregation of the terrain which conducted the movement. This seems to be, in fact, what we have observed in the Colchagua Province (of Chile) as well as in many other cases". The stable variations in spectral content for different site conditions give rise to site dependent ground motion characteristics which result from vertical variations in soil properties (Mohraz, 1976; Seed et al., 1976). These effects have been incorporated into building codes in the United States (UBC; NEHRP, 1991) as well as elsewhere (IAEE, 1992) as site category dependent response spectral shapes. The current UBC site categories (Table 1) and shape coefficients were developed primarily during the ATC-3 effort in the early to mid 1970's and reflect the state of knowledge at that time. Site categories S1 to S3 were developed by Seed et al. (1976) and category S4 was added subsequent to the 1982 Mexico City earthquake to accommodate deep soft (clay) profiles. The site coefficients corresponding to the S1 to S4 site categories affect only the intermediate-to-long period portion of the spectrum (range of approximately constant response spectral velocity) as insufficient data were available to resolve stable features of short period site dependent response. It is important to point out that site dependent spectral shapes reflected in the code provision not only represent ground response spectra, but also accommodate judgmental factors for structural engineering considerations, such

---

<sup>1</sup>Translated from the old Spanish by Professor Ricardo Dobry.

as a factor of 1.25 along with a  $T^{2/3}$  fall-off at long periods.

Subsequent to the 1989 Loma Prieta earthquake and the accompanying dramatic increase of data on site effects, the need was recognized for an update of the code provision site factors. This effort was undertaken by a number of practitioners and culminated in a consensus (1992 NCEER/SEAOC/BSSC/Workshop) set of revised site categories (A to F, Table 1) and a set of both short period ( $F_a$ ) and intermediate-to-long period ( $F_v$ ) site factors applied to the soft rock (Category B) shape. The new site factors accommodate nonlinear site effects through a dependency on soft rock acceleration and velocity based effective accelerations ( $A_a$  and  $A_v$ , Table 2). For these NEHRP proposed revisions, the factor of 1.25 has been changed to 1.2 and the  $T^{2/3}$  spectral decay has been retained. In addition, for categories D, E, and F, at periods shorter than 0.3 sec, the design coefficient is reduced with the multiplicative factor  $1 + 5 T$ . For very long periods ( $> 4$  sec), the design coefficient is increased over the  $T^{2/3}$  decay with a  $T^{4/3}$  decay.

Since the UBC spectra were developed in the early to mid 1970's and the NEHRP recommended revisions are based primarily on site response analyses (categories D and E at rock  $PGA'S \leq 0.1g$  reflect limited empirical analyses) the increase in strong motion data over the last several years provides an important empirical check on these design requirements. The purpose of this project is to provide such an empirical check on the shapes as well as to investigate the benefits of using spectra anchored at two points as in the NEHRP recommended provisions (1994).

## VERIFICATION OF RESPONSE SPECTRAL SHAPES

### Strong Motion Database

The strong motion database available for development of statistical 5% damped response spectral shapes was compiled by Pacific Engineering and Analysis and contains of 98 earthquakes in the magnitude range of about  $M$  5 to  $M$  7.4. The database consists of over 2,000 recordings and most of the available volume 1 records have been reprocessed to extend both the short and long period portions of the motions. Recording sites have been assigned available USGS site codes (Boore et al., 1994). Sites which did not have assigned codes but which had available shear-wave velocity profiles were classified according to the criterion listed in Table 1. Records were assigned UBC site categories based on the following assumption:  $S1 = NEHRP B+C$ ,  $S2 = NEHRP C+D$ , and  $S3 = NEHRP E$ .

For applications to code shapes, the magnitude selection was limited to  $M$  6.3 and above. The breakdown in mean magnitudes, distances, and  $PGA$ 's for each site category is shown in Table 3. Also shown in Table 3 are the number of records (spectra) and earthquakes contributing to each site category. Excluding the near-fault 0 to 10 km shapes, the average magnitude is about 6.75 at a distance of about 35 to 40 km and with a mean  $PGA$  value of about 0.15g.

### Soil Profile Database

To illustrate the type of shear-wave velocity profiles which are implied by the code categories, median and  $\pm 1$  sigma profiles were developed for the UBC and NEHRP generic sites (Figure 1). For UBC sites, as with the strong motion data, it was assumed that  $S1$  is comprised of NEHRP B+C,  $S2$  is comprised of NEHRP C+D, and  $S3$  is equivalent to NEHRP E (Bill Joyner, personal communication). The generic profiles were produced from the Pacific Engineering and Analysis profile database of over 700 shear-wave velocity profiles using the criteria listed in Table 1. NEHRP Site A, which represents very hard rock, is not currently

represented in the profile database. The decrease in overall stiffness as well as variability is quite apparent in going from NEHRP Sites B to E and from UBC Sites S1 to S2.

### UBC Shapes

Figure 2 shows the statistical shapes compared to the UBC code provisions for UBC sites S1, S2, and S3 (two few data were available for site S4) and Table 3 shows the data distributions in  $M$ , distance, and number of records. The UBC spectral shape requirements are shown for both the static (lateral force) and dynamic analyses. The unbiased static provisions, which use a spectral decay of  $T^{-1}$  instead of  $T^{-2/3}$  are also shown. The statistical shapes for S1 and S2 are quite similar, possibly due to the assumed definition of S1 and S2 being overlapping combinations of NEHRP sites B, C, and D. This points out a possible disadvantage of the NEHRP classification scheme in not considering profile depth as part of the criterion. Since profile information rapidly decreases at depths beyond about 70-100 ft, it is very difficult to accurately segregate profiles into depth bins. In general, the UBC shapes are consistent with the ground motion spectra and exceed the median statistical spectra from 0.1 to 10.0 sec.

To assess near fault effects, statistical spectra for site categories S1 and S2 were developed for sites at fault rupture distances of 0 to 10 km (no S3 or S4 sites were available). These results are shown in Figure 2 and suggest that the code shapes (particularly the lateral force requirements) do reasonably well on average for  $M$  in the range of 6.6 to 7.0 (Table 3). However, the S1 dynamic analysis shape is exceeded by the median ground motion at very short periods ( $< 0.08$  sec).

### NEHRP Shapes

The comparisons of the statistical spectra for NEHRP sites B, C, D, and E to the code design shapes are shown in Figure 3. For the code shapes, both the provision requirements, which accommodate structural considerations, and the unbiased spectra are shown. Site A, very hard rock, is not shown as there are currently no sites in the database assigned this category. The spectrum in the NEHRP recommended provisions differs from the UBC spectrum in three major ways. First, the NEHRP reference Category (B) is narrower than the UBC reference category (S1). Second, the spectrum for Category B is anchored at two points instead of one. The short-period portion (periods shorter than approximately 0.5 sec) is anchored to parameter  $A_a$  which is equivalent to the UBC zone factor  $Z$  and represents PGA. The intermediate and long-period portion is anchored to parameter  $A_v$ , which is related to peak ground velocity and is roughly equivalent to spectral acceleration at 1 sec for 5% damping. This concept dates back to the Newmark-Hall (CR-0098) shapes where portions of the design spectra were approximated as two straight lines (in log-log space) with amplitudes proportional to peak ground acceleration and velocity. Third, the NEHRP treatment of site conditions considers nonlinear soil response and affects all portions of the spectrum. The spectra for site categories other B are anchored to  $F_a A_a$  and  $F_v A_v$ , respectively, where  $F_a$  and  $F_v$  are site coefficients that depend on soil category and on ground motion levels  $A_a$  and  $A_v$ , respectively (see Table 2).

To compare statistical shapes to the NEHRP design spectral shapes for each category, it was assumed that  $A_a = A_v$ , which is the case for much of California in the current NEHRP maps. In addition, because the shapes depend upon rock motion amplitude ( $A_a$  and  $A_v$ ) through the  $F_a$  and  $F_v$  factors (Table 2), the data were separated into distance bins based on expected rock PGA ( $A_a$ ) ranges. The expected rock PGA values were computed from a recently developed empirical attenuation relation which classifies rock as NEHRP sites B plus C (Abrahamson and Silva, 1996). In the comparisons shown in Figure 3, site B statistical shapes represents all

distances ( $M > 6.3$ ) since  $F_a$  and  $F_v$  are 1 for all  $A_a$  and  $A_v$ . The mean magnitude is near  $M$  7 with mean distance and PGA of 40 km and 0.15g respectively (Table 3). For sites C, D and E the highest rock PGA ( $A_a$ ) ranges are shown which have sufficient data to constrain shapes ( $\geq 4$  earthquakes and  $\geq 15$  spectra). The C and D sites reflect records selected from distance ranges where the expected rock PGA ranges from about 0.25 to 0.35g for  $M \geq 6.3$ . For these cases  $A_a$  is taken as 0.20g ( $A_v = 0.2$ g) to construct the NEHRP shapes. For site E, to provide enough data for stable statistical shapes, the expected rock PGA range combines the two lowest  $A_a$  and  $A_v$  bins, 0.1 and 0.2g and the expected rock PGA range used was 0.0 to 0.25g.

For sites B and C (Figure 3) the code provision shape exceeds the median statistical shape over the range of 0.1 to 10.0 sec. For site D, the code provision exceeds the statistical shape at long to intermediate periods ( $\geq 0.3$  sec) but is below the data at short periods ( $< 0.3$  sec). For site E, the code provision exceeds the statistical shape but the margin is small at short periods ( $\leq 0.5$  sec).

To assess very high amplitude long period motions, Figure 3 (last plot) compares the NEHRP B shape to the two horizontal components (Professor W. Iwan, personal communication) of the Lucerne site from the  $M$  7.3 1992 Landers earthquake. The site is at a fault distance of 1.1 km and has very high motions on the 260° component (fault normal). Interestingly the code provision shape does extremely well from 0.1 to 10.0 sec. However, it must be emphasized that, since the average recorded PGA at the site is about 0.8g, if the shape had been scaled to an  $A_a = 0.4$ g, the long period absolute level of the 260° component would exceed the code provision by a factor of about 2. In this case, the code provision in absolute level would be close to the average horizontal component at long periods.

As an additional evaluation of the NEHRP provisions, the nonlinear  $F_a$  and  $F_v$  factors were estimated using the empirical attenuation relation of Abrahamson and Silva (1996). In this relation, both rock and soil sites are considered with rock generally reflecting NEHRP B and C (hard rock to very stiff soil) and soil NEHRP C and D (stiff soils). To accommodate this classification, the NEHRP factors ( $F_a$  and  $F_v$ ) were adjusted to reflect ratios of site C + D to site B + C. The empirical  $F_a$  and  $F_v$  factors were computed as ratios (soil/rock) of empirical response spectra, averaged 0.1 to 0.5 sec for  $F_a$  and 0.4 to 2.0 sec for  $F_v$ , for increasing rock PGA values. The results are shown in Table 2 and reflect comparable values for the adjusted NEHRP factors and empirical factors. The empirical  $F_a$  are slightly lower and show a stronger nonlinear effect than the code provision. For  $F_v$ , the empirical show little nonlinear effects while the NEHRP  $F_v$  factors reflect about the same nonlinearity as the NEHRP  $F_a$  factors.

### **PROBABILISTIC SEISMIC HAZARD RESULTS FOR SELECTED CITIES AND COMPARISONS TO CODE SPECTRA**

The purpose of these calculations and the comparisons that follow is to investigate the consistency of the UBC and NEHRP code spectral shapes with the uniform-hazard spectra (UHS) calculated by probabilistic seismic-hazard analysis (PSHA). In particular, we wish to determine to what extent it is necessary to have two spectral anchor points (as in the NEHRP code), in order to accommodate differences in the shape of the UHS that arise from differences in the nature of the seismic threat at different California cities. For instance, one anticipates that the design spectrum for San Francisco should have more low-frequency energy than the one for Los Angeles because more of the hazard at San Francisco comes from large earthquakes in the San Andreas fault. In addition, we wish to investigate the effect of larger uncertainty in the attenuation functions for low frequencies, which tends to flatten the UHS. The interest here is more on the shape of the UHS, rather than on the absolute amplitudes of the code shapes anchor

points.

The source characterizations used for the probabilistic seismic hazard calculations (source geometries, magnitude-recurrence models, maximum magnitude, and their corresponding uncertainties) come from recent published studies performed by others. The source characterization for Los Angeles come from Petersen et al. (1995) and that for San Francisco from Youngs et al. (1994). The source characterization for Sacramento is a combination of the Youngs et al. characterization and USGS (Hansen and Perkins, 1995) sources for the Sacramento region and the Sierra Nevada. Some minor modifications were introduced in these source characterizations, for the sake of simplicity.

The following three attenuation equations for soil were considered: Abrahamson and Silva (1996), Boore et al. (1994), and Sadigh (1988). These attenuation equations apply to UBC soil category S2 and to a mixture of NEHRP soil categories C and D (with a majority of D). These three attenuation equations reflect recent strong-motion data from California and include the effect of fault type (thrust or strike-slip). The Abrahamson and Silva equations also predict different amplitudes for the up-thrown and down-thrown blocks of a thrust fault, but this effect was not considered in the calculations. These two effects are important only for Los Angeles area.

PSHA calculations at the three cities are performed for peak ground acceleration (PGA) and for spectral accelerations ( $S_a$ ) at 0.04, 0.1, 0.2, 0.4, 1, 2, and 4 sec (5% damping). These results are used to construct mean UHSs for 90% non-exceedence probability in 50 years. This exceedence probability (equivalent to an annual exceedence probability of  $2.1 \times 10^{-3}$  or a return period of 475 years) is the one implied in both the UBC and NEHRP codes. In addition, we determine the design earthquakes associated with these hazard results, for both PGA and  $S_a(1 \text{ sec})$ , using McGuire's (1995) procedure. A design earthquake is defined in terms of a magnitude, a distance, and an attenuation-equation  $\epsilon$  (number of standard deviations above the median). Results from the PSHA calculations are shown in Table 4, which also shows the ground-motion amplitudes in the UBC and NEHRP codes, as well as the interim USGS values (Frankel et al., 1995).

The magnitudes and distances that control seismic hazard at these three cities are quite different, as illustrated by the design earthquakes given in Table 4. This is confirmed by Figure 4, which shows the contributions of the various magnitudes, distances, and attenuation  $\epsilon$ s to the mean hazard for PGA and  $S_a(1 \text{ Hz})$ . Local faults (Hollywood, Elysian Park, and others) dominate the hazard in Los Angeles while the San Andreas fault dominates the hazard in San Francisco, as well as the 1 Hz hazard in Sacramento. The local area source dominates the PGA hazard in Sacramento. These differences have an effect on spectral shapes, as will be shown below

Figure 5 compares the mean UHSs obtained from the hazard calculations to the UBC (Category S2) and NEHRP (Categories C and D) spectra for the corresponding cities. The UBC spectrum works well in Los Angeles but under-predicts intermediate- and long-period amplitudes in San Francisco, where higher magnitudes contribute more to seismic hazard. The NEHRP spectrum does not do much better in San Francisco because the NEHRP maps have  $A_h = A_v = 0.4g$ . A more appropriate value of  $A_v$  for San Francisco, together with the two anchor points used by the NEHRP provisions, would provide an adequate fit. The comparisons for Sacramento suggest that the code values for this city are too high. Figure 6 shows comparisons in which the code shapes anchored to values of PGA and  $S_a(1 \text{ sec})$  obtained from hazard results for rock. The UBC spectral accelerations underestimate the UHS at all periods. The NEHRP

spectrum for Category D (the category most representative of the soil attenuation equations) is consistent with the UHS at some periods and is conservative at other periods.

### CONCLUSIONS

Comparison of both UBC and NEHRP design spectral shapes with shapes computed from strong motion recordings at sites with appropriate subsurface conditions suggest that the code provide enveloping criterion including cases for sites within 10 km of the fault rupture. The only exception is for NEHRP site D at short periods ( $\leq 0.3$  sec) where the recorded motions exceed the design shapes.

Comparison of the code spectral shapes to the results from the probabilistic analysis (for 90% non-exceedence probability in 50 years) show that the fixed UBC shape underestimates ground motions by 25 to 50% in San Francisco and Sacramento, respectively, but is adequate for Los Angeles. The more flexible NEHRP shape allows for a better fit to the probabilistic results, but only if both anchoring values ( $A_a$  and  $A_v$ ) are specified appropriately.

### ACKNOWLEDGMENTS

This investigation was funded by the Strong Motion Instrumentation Program, California Division of Mines and Geology. The authors are grateful for this support and wish to thank all members of the SMIP project committee for their very useful comments on the progress of the project. They also wish to thank Mark Petersen, also of CDMG, for providing information on the seismic-source characterization for Los Angeles.

### REFERENCES

- Abrahamson, N.A. and Silva, W.J. (1996). Work in progress.
- Boore, D.M., W.B. Joyner, and T.E. Fumal (1994). "Estimation of response spectra and peak accelerations from western North American earthquakes: and interim report. Part 2. *U.S. Geological Survey Open-File Rept.* 94-127.
- Frankel, A., C. Mueller, T. Barnhard, D. Perkins, E.V. Leyendecker, N. Dickman, S. Hanson, and M. Hopper (1995). "Interim National Seismic Hazard Maps." Internet Web Page, December 15.
- Hansen, S. and D. Perkins (1985). *Seismic Sources and Recurrence Rates as Adopted by USGS Staff for the Production of the 1982 and 1990 Probabilistic Ground Motion Maps for Alaska and the Conterminous United States.* USGS Open-file Report 95-257.
- Mohraz, B. (1976). "A study of earthquake response spectra for different geological conditions." *Bull. Seism. Soc. Am.*, 66(3) 915-935.
- Petersen, M.D., C.H. Cramer, W.A. Bryant, M.S. Reichle, and T.R. Topozada (1995). "Preliminary seismic Hazard Assessment for Los Angeles, Ventura and Orange counties, California Affected by the the January 17, 1994 Northridge Earthquake." submitted to *Bull. Seism. Soc. Am.*, January.
- Seed, H.B., C. Ugas and J. Lysmer. (1976). "Site-dependent spectra for earthquake resistant design." *Bull. Seism. Soc. Am.*, 66(1), 221-243.
- Youngs, R.R., K.J. Coppersmith, C.L. Taylor, M.S. Power, L.A. DiSilvestro, M.L. Angell, N.T. Hall, J.R. Wesling, and L. Mualchin (1992). "A comprehensive Seismic Hazard Model for the San Francisco Bay Area." in *Proc., Second Conference on Earthquake Hazards in the Eastern San Francisco Bay Area*, California Division of Mines and Geology, Special Publication 113.

Table 1 PROFILE TYPES	
UBC	
Soil Profile Type	Description
S <sub>1</sub>	A soil profile with either: (1) rock of any characteristic, either shale-like or crystalline in nature, that has a shear wave velocity greater than 2,500 feet per second or (2) stiff soil conditions where the soil depth is less than 200 feet and the soil types overlying the rock are stable deposits of sands, gravels, or stiff clays.
S <sub>2</sub>	A soil profile with deep cohesionless or stiff clay conditions where the soil depth exceeds 200 feet and the soil types overlying rock are stable deposits of sands, gravels, or stiff clays.
S <sub>3</sub>	A soil profile containing 20 to 40 feet in thickness of soft- to medium-stiff clays with or without intervening layers of cohesionless soils.
S <sub>4</sub>	A soil profile characterized by a shear wave velocity of less than 500 feet per second containing more than 40 feet of soft clays or silts.
NEHRP Provisions	
A	Hard rock with measured shear wave velocity, $\bar{V}_s > 5,000 \text{ ft/sec}$
B	Rock with $2,500 \text{ ft/sec} < \bar{V}_s \leq 5,000 \text{ ft/sec}$
C	Very dense soil and soft rock with $1,200 \text{ ft/sec} < \bar{V}_s \leq 2,500 \text{ ft/sec}$
D	Stiff soil with $600 \text{ ft/sec} \leq \bar{V}_s \leq 1,200 \text{ ft/sec}$
E	A soil profile with $\bar{V}_s < 600 \text{ ft/sec}$ or any profile with more than 10 ft of soft clay
F	Soil requiring site-specific evaluations
Assumed UBC and NEHRP Profile Relationships	
UBC Profile	NEHRP Profile
S1	B and C
S2	C and D
S3	E

Table 2 Fa AND Fv VALUES					
Soil Profile Type	Fa For Shaking Intensity Levels				
	$A_a \leq 0.1$	$A_a = 0.2$	$A_a = 0.3$	$A_a = 0.4$	$A_a \geq 0.50^a$
A	0.8	0.8	0.8	0.8	0.8
B	1.0	1.0	1.0	1.0	1.0
C	1.2	1.2	1.1	1.0	1.0
D	1.6	1.4	1.2	1.1	1.0
E	2.5	1.7	1.2	0.9	b
F	b	b	b	b	b
Soil Profile Type	Fv For Shaking Intensity Levels				
	$A_v \leq 0.1$	$A_v = 0.2$	$A_v = 0.3$	$A_v = 0.4$	$A_v \geq 0.50^a$
A	0.8	0.8	0.8	0.8	0.8
B	1.0	1.0	1.0	1.0	1.0
C	1.7	1.6	1.5	1.4	1.3
D	2.4	2.0	1.8	1.6	1.5
E	3.5	3.2	2.8	2.4	b
F	b	b	b	b	b
<p>Note: Use straight line interpolation for intermediate values of <math>A_a</math> and <math>A_v</math></p> <p><sup>a</sup> Values for <math>A_a, A_v &gt; 0.4</math> are applicable to the provisions for seismically isolated and certain other structure</p> <p><sup>b</sup> Site specific geotechnical investigation and dynamic site response analyses shall be performed.</p>					
Empirical Fa and Fv Values					
Adjusted NEHRP*			Empirical**		
$A_a = A_v$	$F_a$	$F_v$	$F_a$	$F_v$	
0.1	1.3	1.6	1.1	1.5	
0.2	1.2	1.4	1.0	1.4	
0.3	1.1	1.3	0.9	1.4	
0.4	1.1	1.2	0.9	1.4	
0.5	1.1	1.2	0.8	1.4	

\*For site profile C + D relative to profile B + C

\*\*Based on empirical attenuation relation (Abrahamson and Silva, 1996).  $F_a$  averaged from 0.1 - 0.5 sec,  $F_v$  averaged from 0.4 - 2.0 sec.

Site	Number of Records	Number of earthquakes	$\bar{M}$	$\bar{D}$	$\overline{PGA}$ (g)
S1	154	8	6.88	35	0.16
S2	324	12	6.75	33	0.17
S3	100	4	6.72	50	0.10
S1(10)*	12	4	7.00	6	0.72
S2(10)**	40	4	6.62	5	0.41
B	38	5	6.95	40	0.15
C	116	6	6.86	33	0.16
D	208	9	6.68	33	0.18
E	100	4	6.72	49	0.10

\*SMART 1 array at Lotung classified as E.

\*\*Data restricted to closest fault rupture distance  $\leq 10$  km.

City	UBC Z(g)	NEHRP A <sub>s</sub> (g) A <sub>v</sub> (g)	USGS Interim hazard maps <sup>1,2</sup> PGA(g)	Probabilistic Seismic Hazard Analysis <sup>1</sup> (UBC S2, NEHRP C-D soil)	
				PGA(g) S <sub>a</sub> (1Hz) (g)	Design Earthquake
Los Angeles	0.4	0.4 0.4	0.5	0.45 0.55	M 5.9 at 9 km, $\epsilon=1.5$ M 6.5 at 10 km, $\epsilon=0.9$
San Francisco	0.4	0.4 0.4	0.7	0.44 0.73	M 7.7 at 14 km, $\epsilon=0.60$ M 7.7 at 14 km, $\epsilon=0.35$
Sacramento	0.3	0.2 0.3	0.12	0.15 0.22	M 5.1 at 15 km, $\epsilon=1.0$ M 7.8 at 130 km, $\epsilon=1.0$

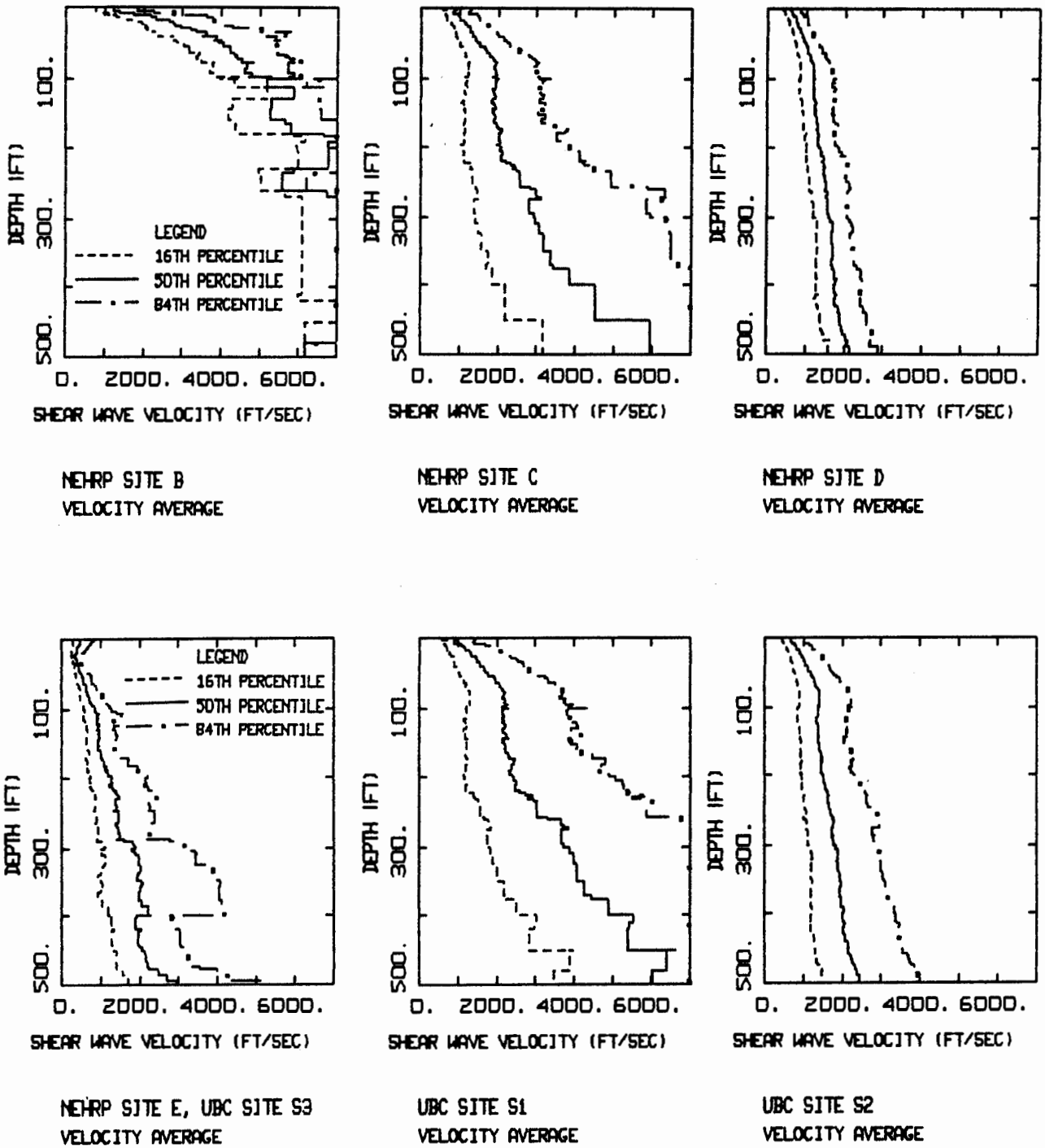


Figure 1. Representative median and  $\pm 1$  sigma shear-wave velocity profiles for the NEHRP provisions and UBC site classes (Table 1) (NEHRP site class A, very hard rock, is currently not represented in the profile database).

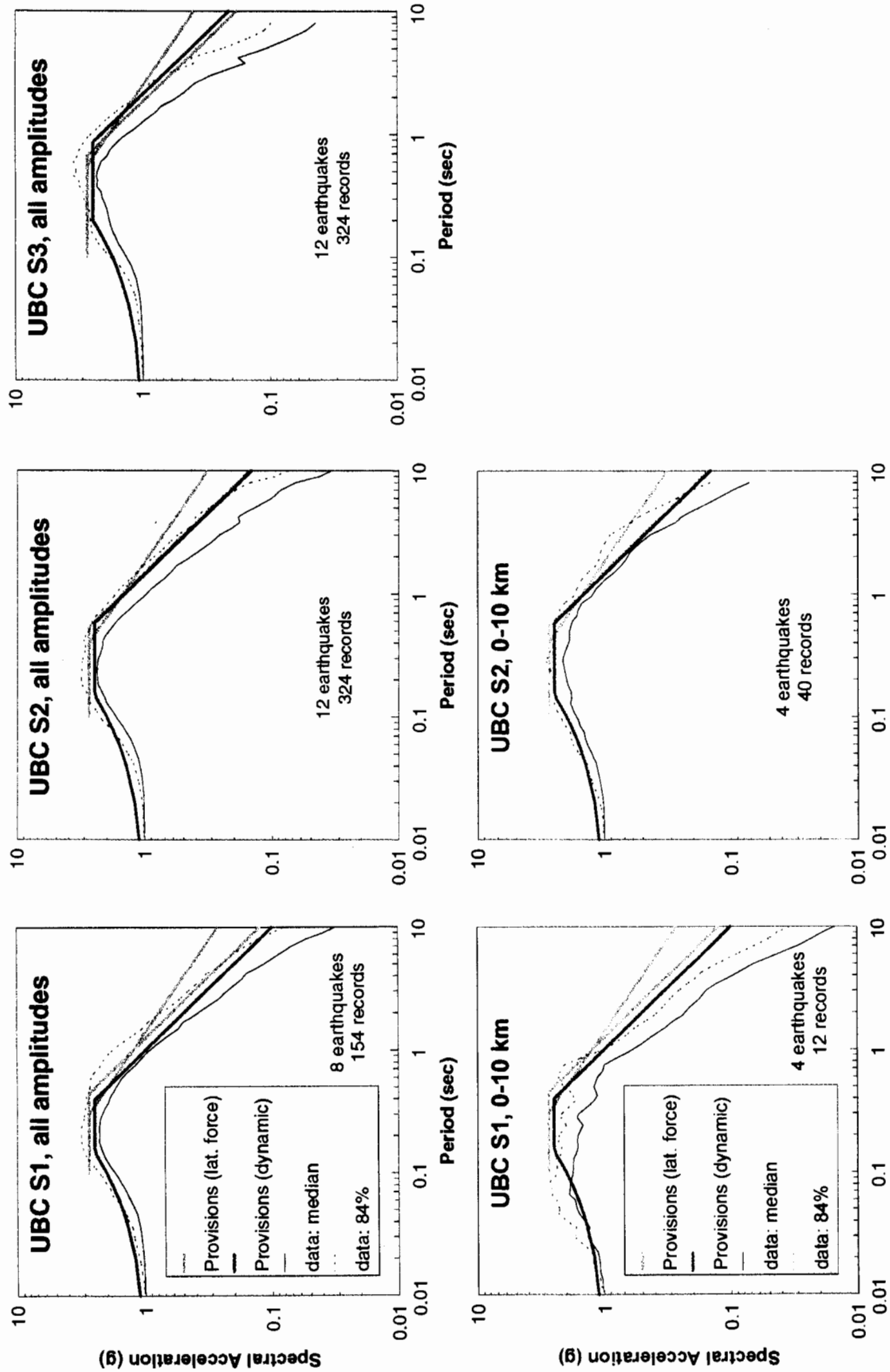


Figure 2. Comparison of UBC code shapes with statistical spectra computed from data recorded at sites classified as S1, S2, and S3 (Table 1). Bottom two figures (S1 and S2) are for sites at fault rupture distances from 0 to 10 km. Site categories S4 and S3 (0 to 10 km) have too few data to provide stable statistical spectra.

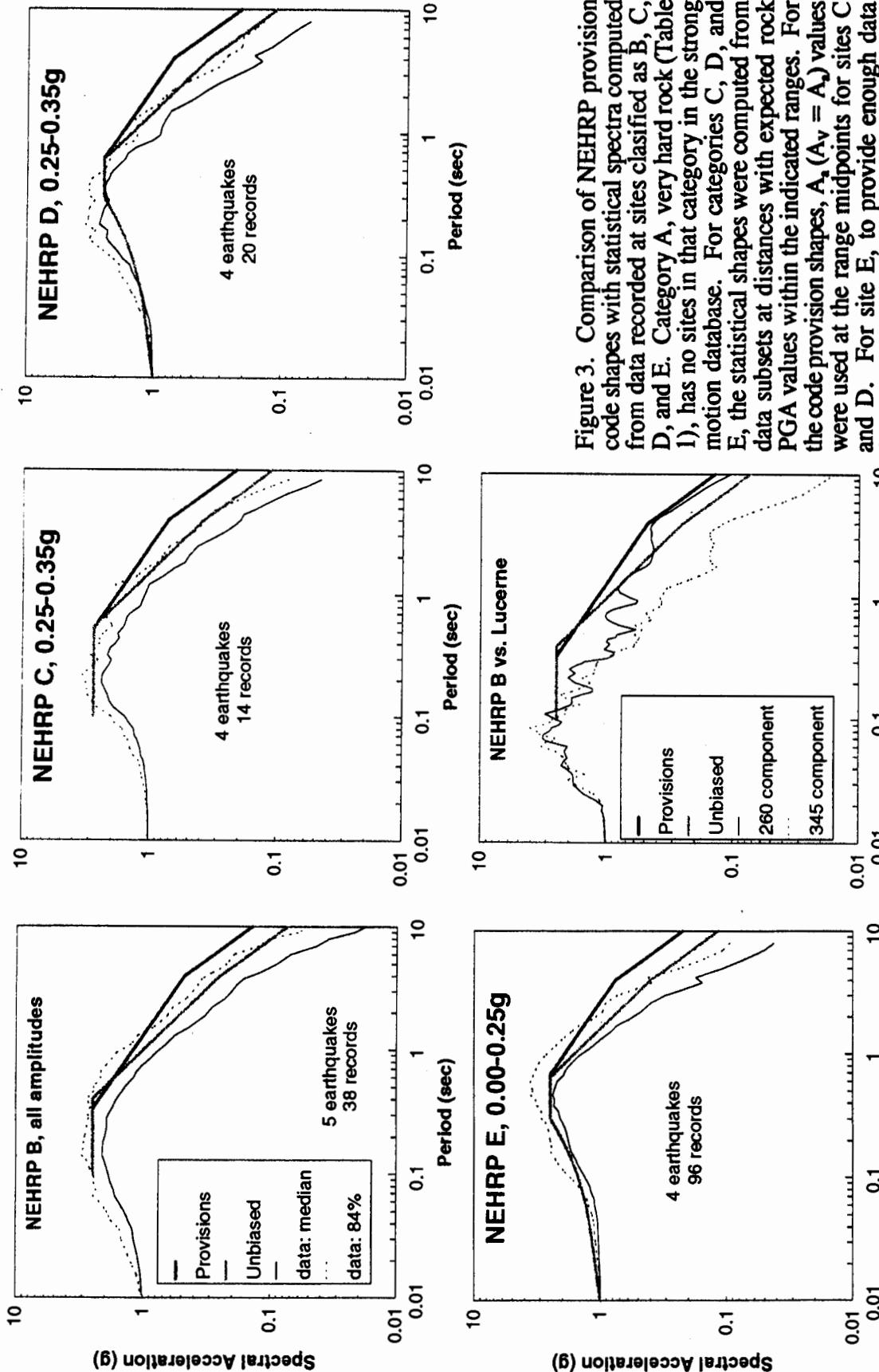


Figure 3. Comparison of NEHRP provision code shapes with statistical spectra computed from data recorded at sites classified as B, C, D, and E. Category A, very hard rock (Table 1), has no sites in that category in the strong motion database. For categories C, D, and E, the statistical shapes were computed from data subsets at distances with expected rock PGA values within the indicated ranges. For the code provision shapes,  $A_s$  ( $A_v = A_s$ ) values were used at the range midpoints for sites C and D. For site E, to provide enough data for stable shapes, records at distances with expected rock PGA values were used along with  $A_s = A_v = 0.15g$ . The ranges were selected to represent the highest motions with sufficient data to constrain the shapes. For site B, since the  $F_a$  and  $F_v$  values are independent of rock motion level ( $A_s$  and  $A_v$ , Table 2), all the site B data (Table 3) were used for the shapes. The final plot compares the Lucerne records for the M 7.3 1992 Landers earthquake (fault distance 1.1 km) to the NEHRP site B shape.

expected rock PGA values in the range of 0.05 to 0.25g were used along with  $A_s = A_v = 0.15g$ . The ranges were selected to represent the highest motions with sufficient data to constrain the shapes. For site B, since the  $F_a$  and  $F_v$  values are independent of rock motion level ( $A_s$  and  $A_v$ , Table 2), all the site B data (Table 3) were used for the shapes. The final plot compares the Lucerne records for the M 7.3 1992 Landers earthquake (fault distance 1.1 km) to the NEHRP site B shape.

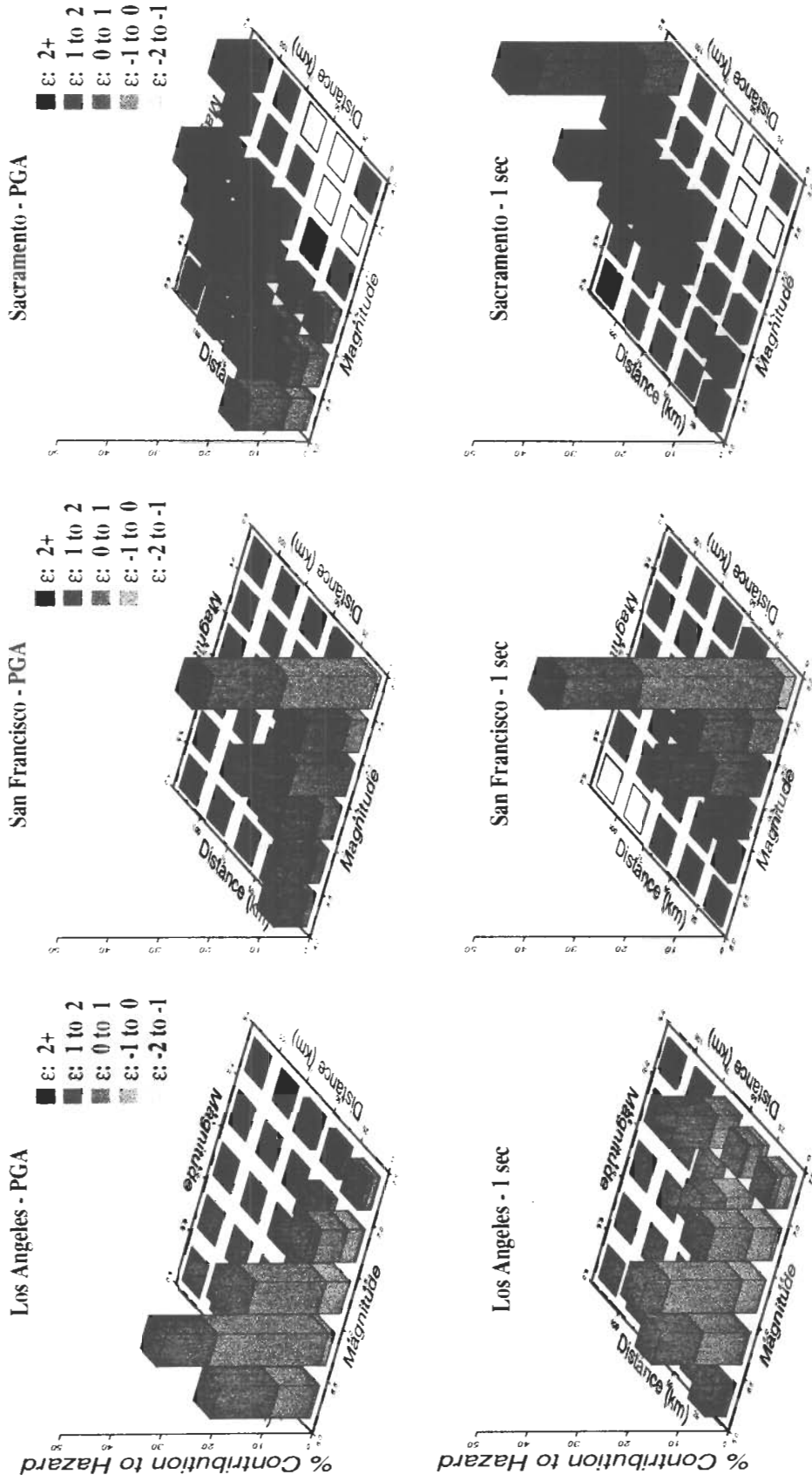


Figure 4. De-aggregation of the mean exceedence probability by magnitude, distance, and ground-motion  $\epsilon$  for the three California cities considered in this study. Non-exceedence probability: 90% in 50 years.

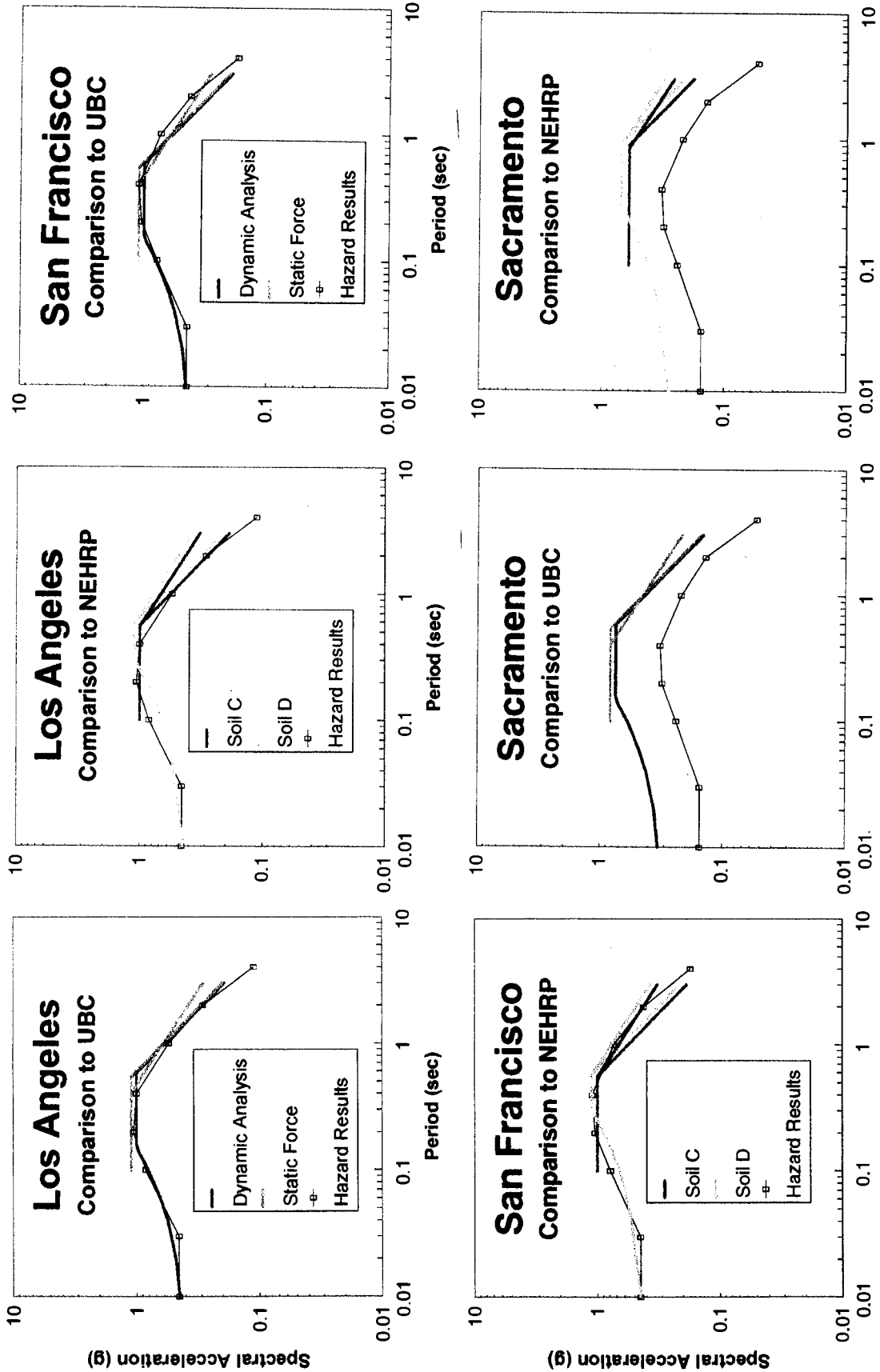


Figure 5. Comparison of UBC and NEHRP spectra for three cities to the corresponding mean uniform-hazard spectra for 90% non-exceedence probability in 50 years.

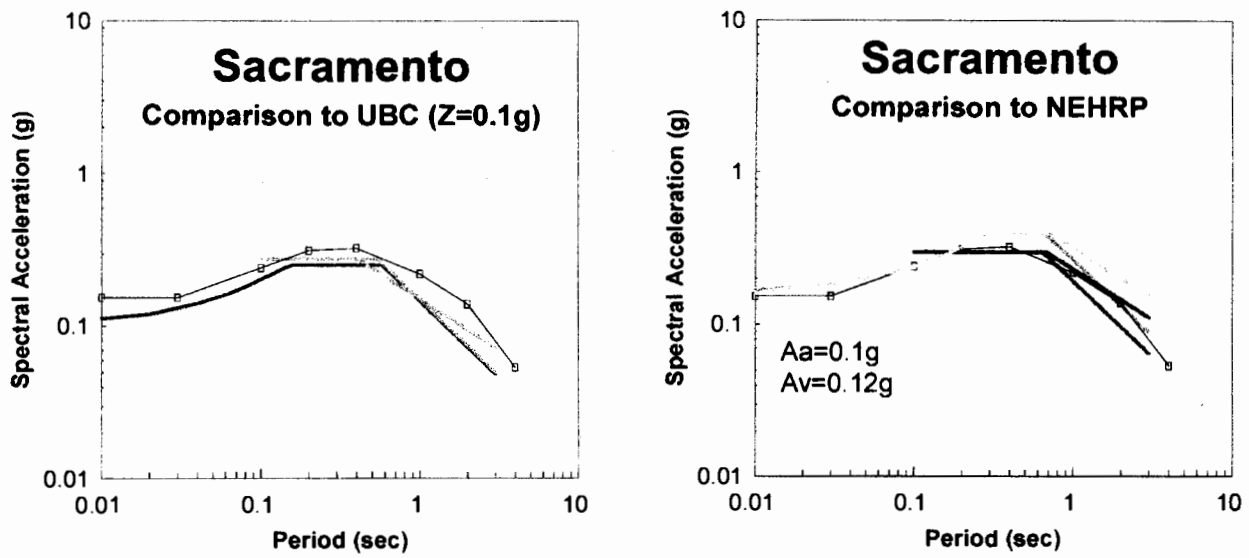


Figure 6. Comparison of UBC and NEHRP spectra for Sacramento to the corresponding mean uniform-hazard spectra for 90% non-exceedence probability in 50 years. Code shapes are anchored to rock seismic-hazard results.

